

# Robust band of critical states in T broken fermionic systems with lattice selective disorder

Eduardo V. Castro\*

*Centro de Física das Universidades do Minho e Porto,  
Departamento de Física e Astronomia, Faculdade de Ciências,  
Universidade do Porto, 4169-007 Porto, Portugal  
CeFEMA, Instituto Superior Técnico, Universidade de Lisboa,  
Av. Rovisco Pais, 1049-001 Lisboa, Portugal and  
Beijing Computational Science Research Center, Beijing 100084, China*

Raphael de Gail, M. Pilar López-Sancho, and María A. H. Vozmediano  
*Instituto de Ciencia de Materiales de Madrid, CSIC,  
Sor Juana Inés de la Cruz 3, Cantoblanco, E-28049 Madrid, Spain*

We analyze the localization properties of two dimensional systems based on partite lattices with a basis. Contrary to standard results, we find that a band of critical states emerges for systems in the unitary class A preserving spin symmetry when disorder is unevenly distributed over the basis atoms. The critical metal arises when the less disordered sublattice is connected and has time reversal symmetry broken. The unexpected robustness to disorder presented here is an appealing result which can be measured in optical lattices.

## I. INTRODUCTION

Anderson localization [1] in one of the best studied phenomena in modern condensed matter. The localization transition in  $d = 2$  depends critically on the symmetry class of the system [2]. In the standard symmetry classification completed with the addition of topological properties [3], the behavior of the unitary class (class A) was initially understood in the context of the quantum Hall effect where the spin degree of freedom is still a good quantum number. It was established numerically that at the center of each Landau level band there is only one critical state – an extended state where the localization length diverges linearly with system size –, indicative of a vanishing  $\beta$  scaling function [4, 5]. The case when both time reversal symmetry  $\mathcal{T}$  and spin rotation symmetry are broken has been the subject of recent investigation [6–9], and the physics was found to be different. It seems well established that a band of extended states, and not a single state, shows up. Depending on the model, this band can be made entirely of critical states [7, 9], or can be a band of truly extended states [6, 7]. Interestingly enough, the transition from the localized side to the critical metal at the energy  $E_c$  is accompanied by a divergent localization length  $\xi(E)$  of the form  $\xi(E) \sim \exp(\alpha/\sqrt{|E - E_c|})$ , reminiscent of a Berezinskii-Kosterlitz-Thouless transition [10]. Critical metallic behavior has also been found in Weyl semimetals [11–13].

In this work we show examples of critical metallic behavior in class A systems with spin rotation symmetry. The critical metal is found on lattices with a basis when disorder is unevenly distributed over the basis atoms. The minimal conditions over the less disordered sublattice for the occurrence of the critical metal are: It has to

be connected and have broken time reversal symmetry.

In all cases we will have a Hamiltonian defined on a lattice with two or more sublattices. Potential (Anderson) disorder is implemented by adding to the Hamiltonian the term  $\sum_{i \in A, B} \varepsilon_i c_i^\dagger c_i$ , with a uniform distribution of random local energies,  $\varepsilon_i \in [-W/2, W/2]$ . For selective disorder we have disorder strength  $W_i$  for sublattice  $i$ .

## II. MODELS AND RESULTS

We will begin by summarizing the situation of the Haldane model [14], a prototype of class A system with spin rotation symmetry. A robust metallic state has already been found by introducing strong selective disorder in one sublattice [15, 16]. The tight binding Hamiltonian can be written as

$$H = -t \sum_{\langle i, j \rangle} c_i^\dagger c_j - t_2 \sum_{\langle\langle i, j \rangle\rangle} e^{-i\phi_{ij}} c_i^\dagger c_j + \Delta \sum_i \eta_i c_i^\dagger c_i(1)$$

where  $c_i = A, B$  are defined in the two triangular sublattices that form the honeycomb lattice. The first term  $t$  represents a standard real nearest neighbor hopping that links the two triangular sublattices. The  $t_2$  term represents a complex next nearest neighbor (NNN) hopping  $t_2 e^{-i\phi_{ij}}$  acting within each triangular sublattice with a phase  $\phi_{ij}$  that has opposite signs  $\phi_{ij} = \pm\phi$  in the two sublattices. This term breaks time-reversal symmetry and opens a non-trivial topological gap at the Dirac points. We have done our calculations for the simplest case  $\phi = \pi/2$ . The last term represents a staggered potential ( $\eta_i = \pm 1$ ). It breaks inversion symmetry and opens a trivial gap at the Dirac points. We use spinless fermions; taking spin into account amounts to a spin degeneracy factor, and lead to the same physics.

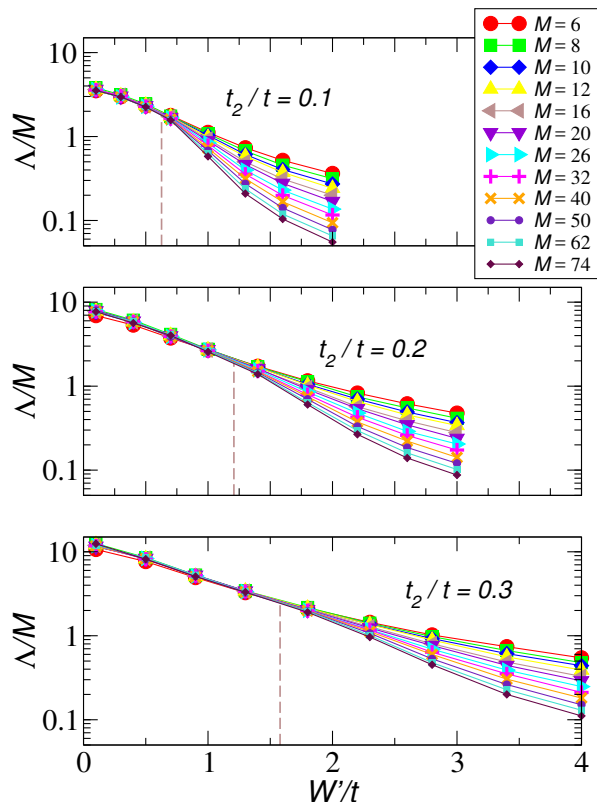


FIG. 1: Normalized localization length  $\Lambda/M$  as a function of disorder strength  $W_B$  in the less disordered (LD) sublattice for various NNN hoppings  $t_2$ , calculated for a long tube with  $M$  unit cells in circumference. The vertical dashed line is a guide to the eye for the transition from critical to localized behaviour. We have fixed the disorder  $W_A = 100t$  and chosen the energy  $E = -0.05t$ .

We have shown previously [16] that disordering a single sublattice, i.e. making  $W_A \neq 0$  but keeping  $W_B = 0$ , a band of critical states appears for  $W_A > W_A^c$  and it is robust no matter how large is the disorder. This result has been established using both a level spacing statistics analysis and the transfer matrix method.

In order to explore the robustness of the metallic state we study its localization behavior with a transfer matrix analysis. We fix the disorder  $W_A = 100t$  and study the metal-insulator transition as a function of  $W_B$  for a given energy inside the band of critical states. We chose  $E = -0.05t$ , and change the disorder strength  $W_B$ . The results are shown in Figs. 1 where we show the normalized localization length  $\lambda/M$  as a function of disorder strength in the less disordered sublattice,  $W_{LD}$ , for various values of the NNN hopping  $t_2$ , calculated for a long tube with  $M$  unit cells in circumference. It is obvious that there is a critical disorder strength  $W_{LD}^c$  below which  $\lambda/M$  does not change with  $M$ , signalling the presence of a critical state. For  $W_{LD} > W_{LD}^c$ , the normalized localization length decreases with  $M$ , as expected for a localized state.

The results above point to the direction that 2D class A systems not always turn into an insulator (trivial or nontrivial) after “levitation and pair annihilation” has occurred between extended states. For systems with more than one sublattice and selective disorder, i.e. at least one sublattice with low disorder below some critical value while the remaining atoms have high disorder, the final state might be a metal. In what follows we try to identify the minimal ingredients needed for such a state to occur.

The main characteristics that we consider relevant for the physics presented in the case of the Haldane model are: 1. The original system has bands with non trivial Berry curvature. 2. After strong selective disorder a “clean sublattice” with full connectivity remains. In the case of the Haldane model it is a triangular lattice with complex NN hopping parameter. 3. The remaining “clean sublattice” has complex hopping parameters that break time reversal symmetry irrespective of the possible global topological triviality of the original lattice.

Next we will present alternative lattice models with a richer sublattice structure where we can discriminate the necessity of these ingredients.

#### 1. Honeycomb lattice with enlarged unit cell models.

In ref. [16] we showed that the critical metal arises in the Haldane model irrespectively of whether the clean limit phase is trivial (non zero Chern number) or topologically non trivial. In any case, the triviality in that case was due to a cancellation of the Chern number upon integration of a non-zero Berry curvature. In order to explore the importance of the Berry curvature on the localization properties of the system we study two different tight-binding models realized in the honeycomb lattice with a tripled unit cell. The basis vectors in real space read  $\mathbf{a}_1 = \frac{3a}{2}(-\sqrt{3}, 1)$  and  $\mathbf{a}_2 = \frac{3a}{2}(\sqrt{3}, 1)$ , and the respective unit cell vectors in reciprocal space are  $\mathbf{b}_1 = \frac{2\pi}{3\sqrt{3}a}(-1, \sqrt{3})$  and  $\mathbf{b}_2 = \frac{2\pi}{3\sqrt{3}a}(1, \sqrt{3})$ . The tight binding Hamiltonian for the two cases we are interested in, can be generically written as

$$H = -t \sum_{\mathbf{r}, \delta} a_{\mathbf{r}}^\dagger b_{\mathbf{r}+\delta} + V \sum_{\mathbf{r}, \delta} a_{\mathbf{r}}^\dagger a_{\mathbf{r}} b_{\mathbf{r}+\delta}^\dagger b_{\mathbf{r}+\delta} + h.c., \quad (2)$$

where  $t$  is the nearest neighbor hopping and  $V$  the nearest neighbor Coulomb repulsion. We use standard notation where  $a_{\mathbf{r}}$  ( $b_{\mathbf{r}}$ ) annihilates an electron at position  $\mathbf{r}$  in sublattice A (B). A mean field analysis of the nearest neighbour Hubbard interaction in this model was studied in refs. [17, 18] to derive spontaneous breaking of time reversal symmetry. Two  $\mathcal{T}$  broken phases TI and TII were found associated to the complex NN hopping distributions shown schematically in fig. 3. With respect to the usual tight binding model for graphene, the T-I phase is just a complex renormalization of the bare hopping plus a Kekule complex distortion. The latter breaks  $\mathcal{T}$  and  $\mathcal{I}$  though preserving their product. According to the analysis in ref. 19 and as shown explicitly in [17, 18], the Berry curvature is identically zero everywhere.

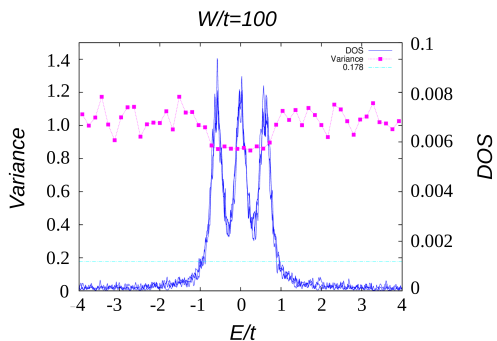


FIG. 2: Level spacing variance of the model TI with disorder distributed over three sublattices. The remaining lattice is not connected and a metallic state does not form.

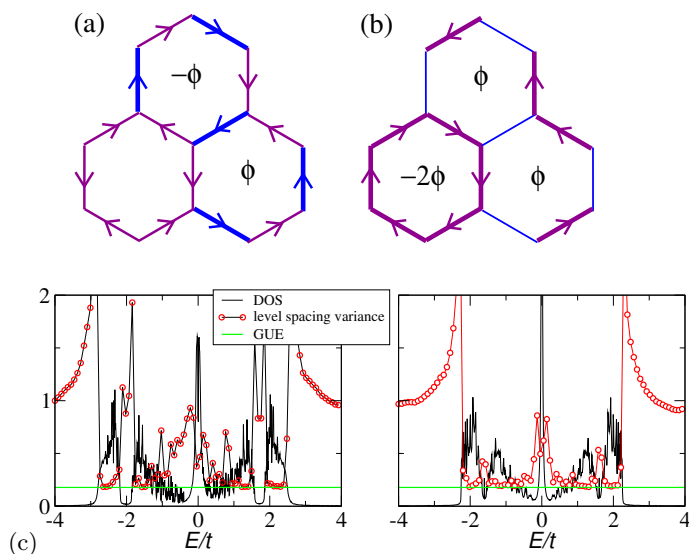


FIG. 3: Schematic representation in terms of effective hoppings and fluxes for phase T-I (a) and TII (b) discussed in the text. (c) Level spacing variance of the model TI and TII showing the appearance of the critical metal for strong selective disorder in one of the six sublattices.

The bands in the TII phase have non-trivial Berry curvature. We have used these models first to establish the necessity of the connectivity of the remaining clean lattice to have an emerging metal. To this purpose, we have studied the level spacing variance of two representative Hamiltonians in the phases TI and TII when selective disorder is acting upon three of the six lattice basis, i. e. , we disorder the sublattices  $A_i$  equally, leaving the sublattices  $B_i$  clean. This disorder distribution is equivalent to the one performed in the Haldane model. In this case, since there is not NNN hopping parameter, the remaining clean sublattice is not connected. The level space variance of the TI model is shown in Fig. 2. As we see, all states are localized. The same occurs with the TII case.

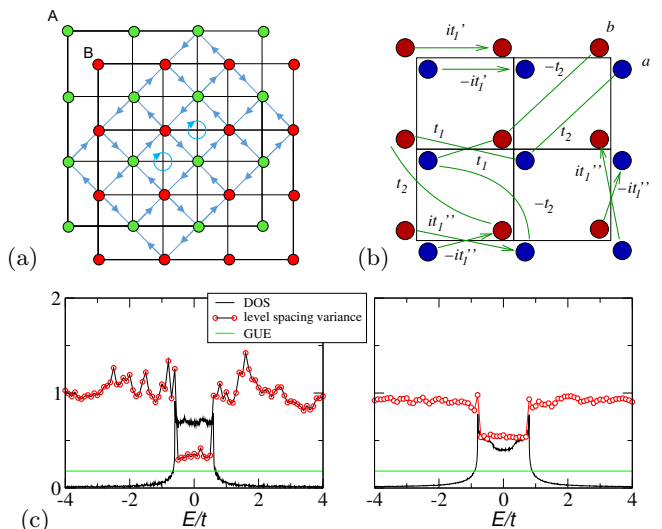


FIG. 4: Schematic representation of the hopping structure of the diatomic (a) and two-orbital model (b) on the square lattice. (c) Level spacing variance of the lattices in the upper part showing standard localization for selective disorder in only one sublattice.

Next, we disorder one of the six sublattices, say sublattice  $A_1$ . We use  $W = 100t$ . The level space variance of both models is shown in the lower part of Fig. 3. As we can see, a metallic phase arises for strong selective disorder of one of the six sublattices. The behavior of the localization length with the size of the lattice points to the fact that, as happened in the Haldane model, the resulting metal is also a critical metal. We have checked that standard (equally distributed among the two sublattices) Anderson disorder induces normal localization in both lattices. The behavior of the TI lattice shows that a non trivial topology is not a necessary condition to support the metallic phase. The next examples will show that the essential property (shared by both TI and TII lattices) is the breakdown of time reversal invariance in the “clean” sublattice.

2. *Square lattice with two orbitals per site and diatomic square lattice.* Our next examples of a simple Chern insulator are supported on the square lattice with two internal degrees of freedom per site that can represent orbital or spin degeneracy  $s = \pm$  [20]. Both tight binding models share the property of having complex NN neighbors and real NNN neighbors. This is the reason why we have chosen them. Upon selective disorder in one sublattice, the remaining clean sublattice will have real hopping parameters and, hence, it will be invariant under time reversal  $\mathcal{T}$ . Both lattices support topologically non trivial phases which will be our starting point.

The Hamiltonian in both cases can be written as

$$H = \sum_{\mathbf{k} \in BZ} c_{\mathbf{k}}^{\dagger} \cdot h_{\mathbf{k}} c_{\mathbf{k}}, \quad (3)$$

$$h_{\mathbf{k}} = 2t_1[\sin k_x \sigma_x + \sin k_y \sigma_y] + [\Delta - 2t_2(\cos k_x + \cos k_y)]\sigma_z.$$

where  $t_1, t_2$  are intra-inter orbital couplings respectively and  $\Delta$  is a staggered potential. A schematic representation of the hopping structure of both lattices is shown in Fig. 4 (upper part). The first example called diatomic square lattice [21, 22] is very similar to the Haldane model: The unit cell has two square plaquettes traversed by a non trivial flux (caused in this case by the NN neighbor hoppings) of opposite signs so that the total flux in the Brillouin zone is zero. The second example is that of the two orbital model on the square lattice. This has been used as an example of a simple tight binding model supporting Chern number bigger than one [23, 24]. A schematic representation of the hoppings is shown in Fig. 4 (upper right part). In this case the fictitious flux induced by the complex hopping parameters per plaquette is zero. Although the two lattices are quite different, the remaining clean sublattice after selective disorder are identical.

We have analyzed the localization behavior of both lattices in the non-trivial topological phase under selective disorder in one sublattice only. Interestingly, despite the non-trivial topology of the bands, these lattices undergo standard Anderson localization upon selective disorder. Their level space variances are shown in Fig. 4 (lower part). There is not any region in energy where the variance reaches the GUE value, so no extended states remain in the spectrum.

### III. DISCUSSION AND SUMMARY

Model	$\Omega$	$\mathcal{T}$ broken	Metal
Haldane	yes	yes	yes
TI	no	yes	yes
TII	yes	yes	yes
Squared bi-orbital	yes	no	no
Squared diatomic	yes	no	no

TABLE I: Summary of the examples given in the text.  $\Omega$  means that the original lattice has non-trivial Berry curvature.  $\mathcal{T}$  broken refers to the clean sublattice that remains after selective disorder.

All the models discussed in this work -except the TI model on the honeycomb lattice - are examples of Chern insulators defined on partite two dimensional lattices.

The objective was to discuss the generality and robustness of the band of critical states found in the Haldane model under strong selective disorder [16]. The results are summarized in Table I. Perhaps the TI case, a topologically trivial, time reversal broken model, is the most significant. Previous studies of localization (or rather *lack of*) established the presence and robustness of extended states carrying the Chern number in topologically non trivial models [6, 9, 25–27] in the class A (absence of any discrete symmetry). The presence of a robust metallic state in the TI lattice leads us to conclude that, irrespective of the topological properties of the original system (first column in table I), the two minimal requirements for the absence of localization upon selective disorder are full connectivity, and time reversal invariance broken in the “clean” sublattice. Absence of localization in the presence of magnetic fields (broken time reversal symmetry) has been analyzed at length in the literature [7, 8, 28] but the hopping structure of the TI model shown in the left hand side of Fig. 3 does not correspond to a magnetic field. The standard localization properties of the topologically non-trivial square lattices shown in Fig. 4 allows us to discard topology as a key point in the absence of localization. As mentioned in the introduction, a band of critical states has been found in models with broken  $\mathcal{T}$  and spin rotation symmetry. The models presented in this work are spin rotation invariant (in fact they are spin-less models) but perhaps the sublattice symmetry plays a similar role as spin rotation (a  $\mathbb{Z}_2$  symmetry in planar systems), broken by the selective disorder.

An important remark about our results refers to the precise nature of the partite lattices considered. The simplest example of a Chern insulator, the Haldane model, is defined in the Honeycomb lattice which is naturally made of two interpenetrating triangular lattices. Selective disorder affects one of the sublattices. When there are internal degrees of freedom, as in the case of the two orbital model in the squared lattice, the selective disorder considered affects an entire *geometrical* sublattice (it destroys both orbitals in nearest neighbour sites). Should we had considered one of the orbitals, say, A (blue in Fig. 4 upper right) as a sublattice, selective disorder of this particular sublattice would led to the diatomic square lattice (Fig. 4 upper left), a Chern insulator with broken  $\mathcal{T}$  and no metallic state.

The findings of this work show that the role of disorder on 2D systems, even if non-interacting, is still far from been fully understood. The experimental advances in optical lattice realizations can shed light on the nature of the critical metal found quite systematically in our  $\mathcal{T}$  broken examples.

We gratefully acknowledge Oscar Pozo for help with the figures. EC acknowledges the financial support of FCT-Portugal through grant No. EXPL/FIS-NAN/1728/2013. This research was supported in part

by the Spanish MECD grants FIS2014-57432-P, the European Union structural funds and the Comunidad de Madrid MAD2D-CM Program (S2013/MIT-3007).

---

\* Electronic address: eduardo.castro@tecnico.ulisboa.pt

- [1] Anderson, P. W. Absence of diffusion in certain random lattices. *Phys. Rev.* **109**, 1492–1505 (1958).
- [2] Abrahams, E., Anderson, P. W., Licciardello, D. C. & Ramakrishnan, T. W. Scaling theory of localization: Absence of quantum diffusion in two dimensions. *Phys. Rev. Lett.* **42**, 673 (1979).
- [3] Schnyder, A. P., Ryu, S., Furusaki, A. & Ludwig, A. W. W. Classification of topological insulators and superconductors in three spatial dimensions. *Phys. Rev. B* **78**, 195125 (2008).
- [4] MacKinnon, A. & Kramer, B. One-parameter scaling of localization length and conductance in disordered systems. *Phys. Rev. Lett.* **47**, 1546 (1981).
- [5] MacKinnon, A. & Kramer, B. The scaling theory of electrons in disordered solids: Additional numerical results. *Z. Phys. B - Condens. Matter* **53**, 1 (1983).
- [6] Qiao, Z. *et al.* Anderson localization from the berry-curvature interchange in quantum anomalous hall systems. *Phys. Rev. Lett.* **117**, 056802 (2016).
- [7] Su, Y., Wang, C., Avishai, Y., Meir, Y. & Wang, X. R. Absence of localization in disordered two-dimensional electron gas at weak magnetic field and strong spin-orbit coupling. *Scientific Reports* **6**, 33304 (2016).
- [8] Wang, C., Su, Y., Avishai, Y., Meir, Y. & Wang, X. R. Band of critical states in anderson localization in a strong magnetic field with random spin-orbit scattering. *Phys. Rev. Lett.* **114**, 096803 (2015).
- [9] Xu, Z., Sheng, L., Xing, D. Y., Prodan, E. & Sheng, D. N. Topologically protected extended states in disordered quantum spin-hall systems without time-reversal symmetry. *Phys. Rev. B* **85**, 075115 (2012).
- [10] Kosterlitz, J. The critical properties of the two-dimensional xy model. *Journal of Physics C: Solid State Physics* **7**, 1046 (1974).
- [11] Sbierski, B., Pohl, G., Bergholtz, E. J. & Brouwer, P. W. Quantum transport of disordered weyl semimetals at the nodal point. *Phys. Rev. Lett.* **113**, 026602 (2014).
- [12] Chen, C.-Z. *et al.* Disorder and metal-insulator transitions in weyl semimetals. *Phys. Rev. Lett.* **115**, 246603 (2015).
- [13] Chen, R., Chen, C.-Z., Sun, J.-H., Zhou, B. & Xu, D.-H. Phase diagrams of weyl semimetals with competing intraorbital and interorbital disorders. *Phys. Rev. B* **97**, 235109 (2018).
- [14] Haldane, F. D. M. Model for a quantum hall effect without landau levels: Condensed-matter realization of the parity anomaly. *Phys. Rev. Lett.* **61**, 2015–2018 (1988).
- [15] Castro, E. V., López-Sancho, M. P. & Vozmediano, M. A. H. Anderson localization and topological transition in chern insulators. *Phys. Rev. B* **92**, 085410 (2015).
- [16] Castro, E. V., de Gail, R., López-Sancho, M. P. & Vozmediano, M. A. H. Absence of localization in a class of topological systems. *Phys. Rev. B* **93**, 245414 (2016).
- [17] Castro, E. V. *et al.* Topological fermi liquids from coulomb interactions in the doped honeycomb lattice. *Phys. Rev. Lett* **107**, 106402 (2011).
- [18] Grushin, A. G. *et al.* Charge instabilities and topological phases in the extended hubbard model on the honeycomb lattice with enlarged unit cell. *Phys. Rev. B* **87**, 085136 (2013).
- [19] Sun, K. & Fradkin, E. Time-reversal symmetry breaking and spontaneous anomalous hall effect in fermi fluids. *Phys. Rev. B* **78**, 245122 (2008).
- [20] Wu, Y.-L., Bernevig, B. A. & Regnault, N. Zoology of fractional chern insulators. *Phys. Rev. B* **85**, 075116 (2012).
- [21] Hou, J.-M. Hidden-symmetry-protected topological semimetals on a square lattice. *Phys. Rev. Lett.* **111**, 130403 (2013).
- [22] Ostahie, B., Niță, M. & Aldea, A. Edge-state mechanism for the anomalous quantum hall effect in a diatomic square lattice. *Phys. Rev. B* **98**, 125403 (2018).
- [23] Prodan, E., Hughes, T. L. & Bernevig, B. A. Entanglement spectrum of a disordered topological chern insulator. *Phys. Rev. Lett.* **105**, 115501 (2010).
- [24] Grushin, A. G., Neupert, T., Chamon, C. & Mudry, C. Enhancing the stability of a fractional chern insulator against competing phases. *Phys. Rev. B* **86**, 205125 (2012).
- [25] Pruisken, A. The integral quantum hall effect: Shortcomings of conventional localization theory. *Nucl. Phys. B* **295**, 253 (1988).
- [26] Ludwig, A. W. W., Fisher, M. P. A., Shankar, R. & Grinstein, G. Integer quantum hall transition: An alternative approach and exact results. *Phys. Rev. B* **50**, 7526 (1994).
- [27] Werner, M. A., Brataas, A., von Oppen, F. & Zaránd, G. Anderson localization and quantum hall effect: Numerical observation of two-parameter scaling. *Phys. Rev. B* **91**, 125418 (2015).
- [28] Kleinert, P. & Bryksin, V. V. Microscopic theory of anderson localization in a magnetic field. *Phys. Rev. B* **55**, 1469–1475 (1997).